American Journal of Materials Science. 2011; 1(1): 57-66
DOI: 10. 5923/j. materials.20110101.09

Initial Stage Growth Mechanism of $LaFeO_3$ Perovskite through Magnetomechanical Ball-Milling of Lanthanum and Iron Oxides

Monica Sorescu*, Tianhong Xu, Alex Hannan

Department of Physics, Duquesne University, Pittsburgh, 15282, USA

Abstract The initial stage growth mechanism of $LaFeO_3$ perovskite has been investigated using magnetomechanical milling of La_2O_3 and Fe_2O_3. X-ray diffraction, differential scanning calorimetry and thermogravimetry analysis, Mössbauer and optical diffuse reflectance spectroscopy were combined to study the phase evolution of the composites during the milling process. The XRD results showed that La_2O_3 is unstable and converted to $La(OH)_3$. No reaction between $La(OH)_3$ and Fe_2O_3 took place when the milling time was less than 25 hours. The $LaFeO_3$ was detected only when the milling time was around 50 hours for shear and 25 hours for impact mode, respectively. The DSC-TGA results suggested a two-step dehydration of $La(OH)_3$. The Mössbauer spectra of the composites consisted of two sextets and one doublet, indicating the La^{3+} substitution of Fe^{3+} into the Fe_2O_3 lattice and the Fe^{3+} substitution of La^{3+} into the $La(OH)_3$ lattice. The formation of $LaFeO_3$ occurs between nano-sized La^{3+} substituted/un-substituted Fe_2O_3 and LaOOH.

Keywords Magnetomechanical Ball-Milling, Perovskite Oxide, X-Ray Diffraction, Mössbauer, Simultaneous DSC-TGA

1. Introduction

ABO_3-type perovskite materials have attracted considerable attention due to their wide applications, such as catalysts[1,2], gas sensing materials[3,4], magnetic materials[5], fuel cell materials[6,7], and electric ceramic materials[8,9]. Up to now, many routes have been developed to synthesize $RFeO_3$-type perovskite materials (R stands for rare earth metal), such as the conventional method based on the solid state reaction between R_2O_3 and Fe_2O_3 at high temperature [10], the sol-gel combustion method[11], and the glycine-nitrate process method[12]. The complication in solid state reaction to produce single phase $LaFeO_3$ lies mainly in how to mix the reactants homogeneously. Otherwise, the high reaction temperature is required and second phase often exists in the prepared composite oxides. To obtain pure $LaFeO_3$, it has been reported that calcination at 1000°C for 184 hours is needed, and X-ray diffraction patterns with shorter periods of calcination time still show peaks of La_2O_3 and Fe_2O_3 phases that do not completely react[13]. Even in the sonochemical method, crystalline $LaFeO_3$ can only be observed by calcining the precursor at 800°C in air for 24 hours, additionally, this method utilizes expensive reactants [14]. The catalytic activity and the gas sensing characteristics of $LaFeO_3$ are strongly dependent on the particle size [15,16], and the calcinations at high temperature for long periods of time increase the average particle size and decrease the surface area, which in turn limits the potential application of $LaFeO_3$ as catalyst and gas sensor.

For catalytic applications of $LaFeO_3$ based materials, two main factors are mostly considered, such as the typical crystalline structure and large surface area[17]. High energy ball milling is a well established method for preparing amorphous, composite and nanocrystalline materials with high surface area and interesting defects. This preparation method is promising for use at a production scale due to its relatively low cost and simple operation.

Kaliaguine et al. have reported the process for synthesizing ABO_3-type perovskite using high energy ball milling, the obtained materials showed high surface area and high defect density, and the improved catalytic activity in volatile organic compounds (VOC) oxidation[18,19]. Recently, Zhang et al.[20] have employed the mechanochemical method to synthesize the $RFeO_3$ at room temperature using R_2O_3 and Fe_2O_3 as reactants (R = La, Nd, Sm). However, the magnetic properties were not studied. Cristóbal et al. [21] also synthesized the $LaFeO_3$ using high-energy milling of La_2O_3 and Fe_3O_4 or Fe_2O_3; the magnetic properties of the obtained materials were measured by vibration sample magnetometry and showed significant ferromagnetic components due to the spin-canting effect induced by the me-

* Corresponding author:
sorescu@duq.edu (Monica Sorescu)
Published online at http://journal.sapub.org/ materials

chanochemical treatment. However, the growth mechanism of $LaFeO_3$ with different starting reactants (Fe_3O_4 and Fe_2O_3) was not fully discussed, and an extra step, calcinations of hygroscopic La_2O_3 at 1000°C for 2 hours, was introduced. Recently, Mössbauer spectroscopy was used to characterize the magnetic properties of the as-obtained systems, especially the substitution between transition metal ions and Fe^{3+} into α-Fe_2O_3 and the transition metal oxides lattices at atomic resolution. However, the conventional ball milling is highly energetic, and the solid state reactions normally take place at very short time periods. Therefore, it is very difficult to trace the structural transformation and reaction mechanism during the milling processes. It has been demonstrated that the magneto-mechanical milling can be used to synthesize magnetic systems with low values of impurities, which is very important for understanding the initial stage of reaction mechanism.

In this work, the initial stage growth mechanism of $LaFeO_3$ perovskite is investigated using the low energetic magnetomechanical milling of La_2O_3-Fe_2O_3 mixtures in 1:1 ratios at room temperature. X-ray diffraction, simultaneous DSC-TGA, Mössbauer spectroscopy and UV-Vis spectroscopy are employed to study phase information, thermal behavior and magnetic properties of composite oxides at different durations of milling time. The growth mechanism of $LaFeO_3$ in connection with phase evolutions of the Fe_2O_3 and La_2O_3 under magnetomechanical milling process is discussed.

2. Experimental

Lanthanum and iron oxides were commercially purchased from Alfa Aesar: lanthanum oxide (99.99% metals basis, average particle size about 60nm), and iron oxides (α-Fe_2O_3, 99% metal basis, average particle size about 48nm). For magnetic milling, powders of lanthanum and iron oxides (total mass 40 g for shear and impact mode, respectively, molar ratio 1:1) were placed into the vial of a magneto-mill Uni-ball-mill 5. The milling modes in this mill could be easily adjusted from the low-energy shear to the high-energy impact. In the shear mode, the balls both rotate and oscillate around an equilibrium position at the bottom of the milling cylinder in a strong magnetic field (0.4 T). In the impact mode, the ball movement during the milling process is confined to the vertical plane by the cell walls and is controlled by the external magnetic field. In both cases, the magnetic field is provided by FeNdB magnets. The intensity and direction of the magnetic field can be externally adjusted, allowing the ball trajectories and impact energy to be varied in a controlled manner.

The X-ray diffraction patterns of samples were obtained using a PANalytic X'Pert Pro MPO diffractometer with CuK_α radiation (45kV/40mA, λ = 1.54187 Å) with a nickel filter on the diffracted side. A silicon-strip detector called X'cellerator was used. The scanning range was 10 - 80º (2θ) with a step size of 0.02º. The average particle size was determined by the Scherrer method. The lattice parameters were extracted from Rietveld structural refinement of the XRD patterns.

Simultaneous DSC-TGA experiments were performed using a Netzsch Model STA 449 F3 Jupiter instrument with a Silicon Carbide (SiC) furnace. Samples were contained in a manufacturer's alumina crucible with an alumina lid. Series of experiments were performed using 20 ± 2 mg sample size. The atmosphere consisted of flowing protective argon gas at a rate of 50ml/min. DSC and TGA curves were obtained by heating samples from room temperature to 800ºC with a ramp rate of 10ºC/min. Both DSC and TGA curves were corrected by subtraction of a baseline which was run under identical conditions as the DSC-TGA measurement with residue of samples in the crucible. The Netzsch Proteus Thermal Analysis software was used for DSC and TGA data analysis.

Room temperature transmission Mössbauer spectra were recorded using an MS-1200 constant acceleration spectrometer with a 10mCi ^{57}Co source diffused in Rh matrix. Least-squares fittings of the Mössbauer spectra were performed with the NORMOS program.

Optical diffuse reflectance spectra were obtained using a Varian Cary 5000 UV/Vis/NIR spectrophotometer. The sample was loaded into a Harrick Praying Mantis diffuse reflectance accessory that uses elliptical mirrors. $BaSO_4$ was used as a 100% reflectance standard. Scans were performed from 2500 to 200nm at a rate of 600nm/min, wavelength data were converted to electron volts, and the percent reflectance data were converted to absorbance units using the Kubelka–Munk equation[22].

3. Results and Discussion

3.1. X-Ray Diffraction

Figure 1 shows the evolution of XRD patterns of mixed lanthanum and iron oxides at different milling times for the shear mode. The starting materials are pure Fe_2O_3 and La_2O_3; however, due to the highly hygroscopic characteristics of La_2O_3, the La_2O_3 converts to $La(OH)_3$ when the

Fe_2O_3 and La_2O_3 are milled for very short time. This was confirmed by the XRD pattern of 2 h milled mixture of Fe_2O_3 and La_2O_3 (Figure 1a). The diffraction peaks of $La(OH)_3$ have much stronger intensities comparing to those of the Fe_2O_3 phase. No La_2O_3 phase was detected, indicating that all of La_2O_3 phase was converted to $La(OH)_3$ phase for La-containing components; La_2O_3 is highly instable when exposed to air after very short milling time. The presence of Fe_2O_3 and absence of $Fe(OH)_3$ diffraction peaks also suggests that Fe_2O_3 is relatively stable in air.

As the milling progresses, the diffraction peak intensities of the starting materials Fe_2O_3 and $La(OH)_3$ decrease slightly for milling times of 4, 8, and 12 h respectively, suggesting the slight decrease in particle sizes of both starting materials under the low energetic shear mode milling process. Especially, after 25 hours of milling time (Figure

1e), the diffraction peak intensities of both Fe_2O_3 and $La(OH)_3$ decreased dramatically and the peaks broadened as well, indicating the longer ball milling time causes further decrease in particle size of the starting materials. The average particle sizes of the Fe_2O_3 and $La(OH)_3$ were estimated to be ~ 25nm and ~ 21nm, respectively. $La(OH)_3$ and Fe_2O_3 are still the phases which could be detected, suggesting there is no occurrence of solid state reaction to form $LaFeO_3$ phase at this milling time scale.

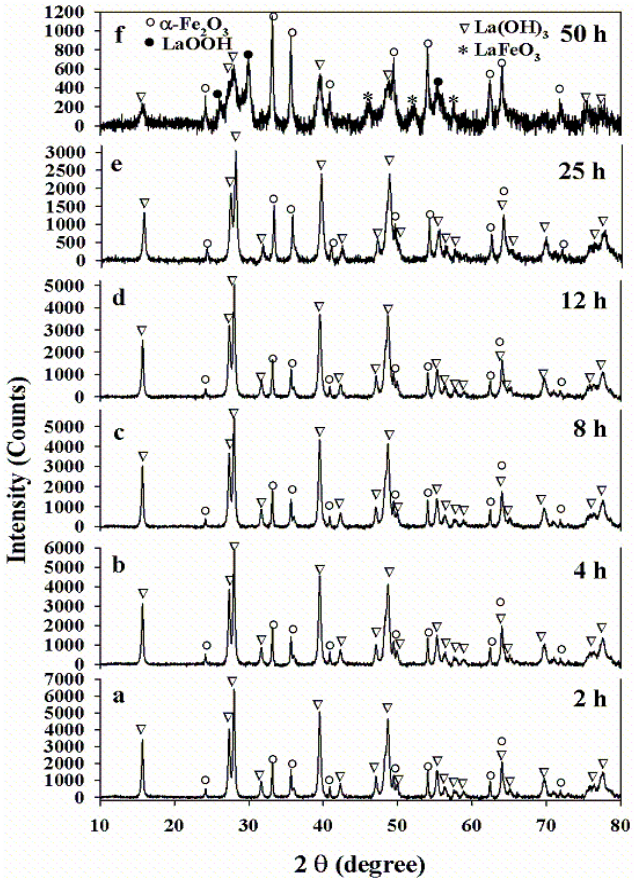

Figure 1. XRD patterns of mixed La_2O_3-α-Fe_2O_3 samples in 1:1 molar ratio under shear mode and milling time of: (a) 2 hours; (b) 4 hours; (c) 8 hours; (d) 12 hours; (e) 25 hours; (f) 50 hours, respectively.

After 50 h of milling time (Figure 1f), dramatic phase evolutions occur. First of all, the diffraction peaks corresponding to $La(OH)_3$ and Fe_2O_3 are still present, but the peak intensities decrease dramatically, indicating the further decreases in average particle sizes of the $La(OH)_3$ and Fe_2O_3. On the other hand, the XRD diffraction peaks corresponding to the $LaFeO_3$ (JCPDS No.: 37-1493) phase could be observed (Figure 1f), indicating the occurrence of the solid state reaction between Fe_2O_3 and/or $La(OH)_3$ related phase. The diffraction peaks of $LaFeO_3$ phase are very broad, suggesting the formed $LaFeO_3$ phase is amorphous with the average particle size less than 10nm. The most interesting observation is the appearance of the lanthanum oxyhydroxide phase (LaOOH), which has not been observed during the conventional milling process. The LaOOH phase is due to the dehydration of $La(OH)_3$ under the magneto-mechanical milling process. Comparing with the conventional ball milling, the magneto-mechanical milling possesses lower energy and it may only covert the $La(OH)_3$ phase to intermediate LaOOH phase. The conventional milling, with much higher energy and faster ball-rotation speed, may convert $La(OH)_3$ phase to La_2O_3 phase directly, therefore, no intermediate LaOOH phase is observed. The further evidence is confirmed by the two-step dehydration of $La(OH)_3$ phase in the next DSC-TGA measurement. The average particle sizes of both LaOOH and $LaFeO_3$ phases are smaller than 10nm as estimated from Scherrer equation, suggesting the formation of $LaFeO_3$ phase may occur between nano-sized Fe_2O_3 and LaOOH, and the average particle size of starting materials is smaller than 10nm to initiate this type of solid state reaction under milling process.

Figure 2 shows the evolution of XRD patterns of mixed lanthanum and iron oxides at different milling times for impact mode. Similar XRD pattern evolutions as a function of milling time were obtained as those of samples milled under shear mode and the average particle sizes of both $La(OH)_3$ and Fe_2O_3 decrease with the milling time. However, there are still some differences in XRD patterns between shear and impact modes. For the more energetic impact mode, four phases are present after 25 hours of milling time (Figure 2e), Fe_2O_3, $La(OH)_3$, traces of LaOOH and $LaFeO_3$ perovskite phases. The earlier appearance of LaOOH and $LaFeO_3$ phases is in good agreement with the fact that the impact mode is more energetic than the shear mode. Similar to the shear mode, the formed $LaFeO_3$ phase is amorphous, with broad and low intensities in the XRD diffraction peaks. Both the LaOOH and $LaFeO_3$ perovskite phases have the average particle sizes smaller than 10nm, while the average particle size of $La(OH)_3$ is ~ 20nm. This confirms our previous assumption that the formation of $LaFeO_3$ perovskite may occur between nano-sized Fe_2O_3 and LaOOH. After 50 hours of milling time under impact mode (Figure 2f), the diffraction peak intensities of LaOOH and $LaFeO_3$ phases increase. This suggests the growth of the $LaFeO_3$ and further dehydration of $La(OH)_3$ under longer milling time. The diffraction peak intensities of Fe_2O_3 decrease, suggesting the consumption of Fe_2O_3 as well as further decrease in average particle size of Fe_2O_3 phase. Interestingly, no $La(OH)_3$ phase is observed, which is different from low energetic shear milling mode, suggesting that all of the $La(OH)_3$ phase converts to LaOOH phase under higher energetic milling process, besides the formation of $LaFeO_3$ perovskite. LaOOH was also obtained as intermediate product from the thermal transformation of $La(OH)_3$ at 330°C[23], can be synthesized using an electrochemical method[24], and it completely changes to $La(OH)_3$ within 48 h in ambient atmosphere by water absorption.

No La_2O_3 phase was detected during studied milling time range (from 0 to 50 hours) for both shear and impact modes, indicating that it is not a necessary step for $La(OH)_3$ and/or LaOOH to dehydrate to La_2O_3 and then to produce $LaFeO_3$ perovskite under milling process. The simultaneous appearance of LaOOH and $LaFeO_3$ phases and the similar particle sizes also suggested that the solid state reaction to

form $LaFeO_3$ occurs between nanosized LaOOH and La^{3+} partially substituted/un-substituted Fe_2O_3.

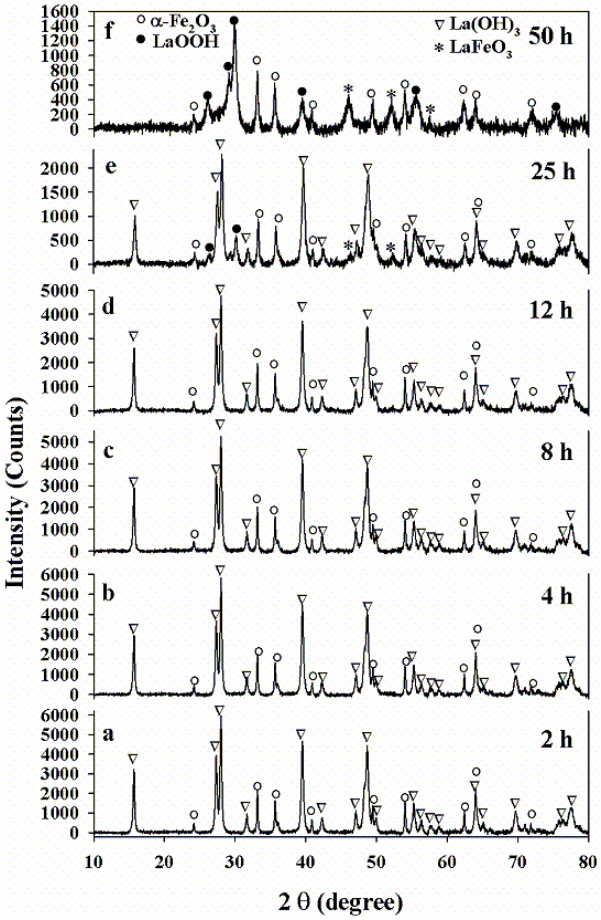

Figure 2. XRD patterns of mixed La_2O_3-α-Fe_2O_3 samples in 1:1 molar ratio under impact mode and milling time of: (a) 2 hours; (b) 4 hours; (c) 8 hours; (d) 12 hours; (e) 25 hours; (f) 50 hours, respectively.

3.2. Simultaneous DSC-TGA

Simultaneous DSC-TGA experiments have been used to study the solid-solid interaction of mixed TiO_2-Fe_2O_3 systems and thermal behavior of precursors of the $LaFeO_3$ perovskite-type composite oxides nanocrystals[25,26]. Differential thermal analysis (DTA) was also employed to study the thermal behavior of Fe_2O_3 + 3Al + Fe powder mixture under different milling times[27]. It was found that the milling process has a great effect on the thermal behavior of the mixed oxide systems and nanocomposite powder.

Figures 3 and 4 display the simultaneous DSC-TGA curves of mixed starting materials after different milling times for shear and impact modes, respectively. For the 2 h milled sample under the shear process (Figure 3a), two endothermic peaks can be clearly observed from the DSC measurement, with peak temperatures at 367 and 527°C, respectively. The thermal behavior of the 2 h milled sample was simultaneously investigated using TGA analysis (Figure 3g). The thermogravimetry reveals two major weight losses: one is in a relatively low temperature range from 300°C to 385°C, with a weight loss of -6.45% and the other starts at 450°C and ends at 530°C, with a weight loss of -2.94%. These two weight losses are due to the dehydration of $La(OH)_3$, which was formed when La_2O_3 was exposed to air and absorbed moisture. These two weight losses are in good agreement with the DSC curve for this sample, which shows two endothermic peaks. The peak temperatures of 367 and 527°C on the DSC curve are exactly at the centre of the TGA curve where the two weight losses occur. The first weight loss of 6.45% between 300 and 385°C is consistent with the conversion of $La(OH)_3 \rightarrow$ LaOOH (theoretical value 6.69%) considering the presence of Fe_2O_3, while the second weight loss of 2.94% corresponds to the further dehydration of LaOOH to form La_2O_3. The relative ratio of these two weight losses is about ~ 2.19, in good agreement with the two-step dehydration processes of $La(OH)_3 \rightarrow$ LaOOH $\rightarrow$ La_2O_3 with theoretical relative weight loss ratio of 2.

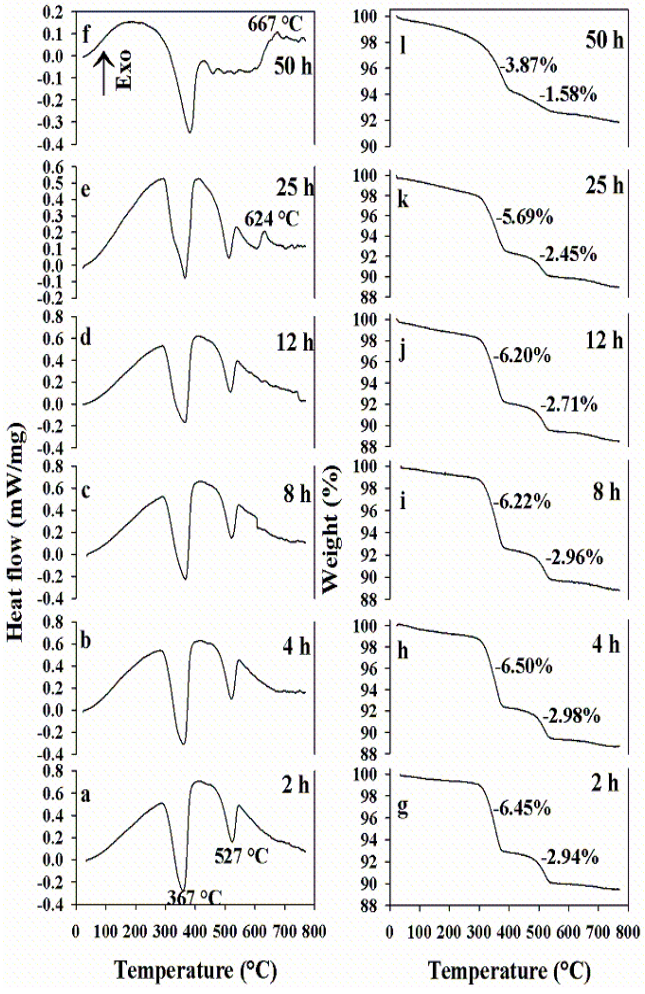

Figure 3. DSC curves of mixed La_2O_3-α-Fe_2O_3 samples in 1:1 molar ratio under shear mode and milling time of: (a) 2 hours; (b) 4 hours; (c) 8 hours; (d) 12 hours; (e) 25 hours; (f) 50 hours, and TGA curves of mixed La_2O_3-α-Fe_2O_3 samples in 1:1 molar ratio under shear mode and milling time of: (g) 2 hours; (h) 4 hours; (i) 8 hours; (j) 12 hours; (k) 25 hours; (l) 50 hours, respectively.

XRD analysis of the residue of the 2 h milled sample after DSC-TGA measurements shows there is no detectable $LaFeO_3$ phase after heat treatment up to 800°C. Therefore, the wide exothermic band on the DSC curve of the 2 h

milled La_2O_3-Fe_2O_3 sample in the studied temperature range can be assigned to the crystallization of the starting materials under heat treatment.

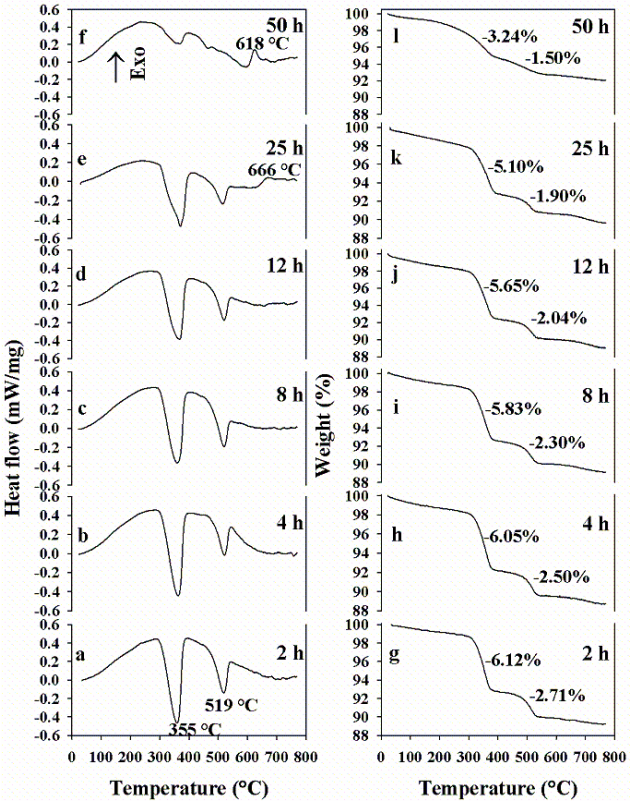

Figure 4. DSC curves of mixed La_2O_3-α-Fe_2O_3 samples in 1:1 molar ratio under impact mode and milling time of: (a) 2 hours; (b) 4 hours; (c) 8 hours; (d) 12 hours; (e) 25 hours; (f) 50 hours, and TGA curves of mixed La_2O_3-α-Fe_2O_3 samples in 1:1 molar ratio under impact mode and milling time of: (g) 2 hours; (h) 4 hours; (i) 8 hours; (j) 12 hours; (k) 25 hours; (l) 50 hours, respectively.

As the milling progresses in the time range of 4 to 25 h, two endothermic peaks on DSC curves and the corresponding two weight losses can still be seen (Figure 3b-e and Figure 3h-k), suggesting the presence of $La(OH)_3$ phase, which is consistent with the XRD results. Through the analysis of the percentage values of the two weight losses, it can be observed that the two values for each sample decrease as a function of milling time. The slight decreases in the intensities of the two endothermic peaks on DSC curves and the two corresponding weight losses may suggest that part of the $La(OH)_3$ enters the Fe_2O_3 lattice, with the release of water during the milling processes. There is a small exothermic peak at 624°C for 25 h milled sample (Figure 3e), which can be assigned to the formation of $LaFeO_3$ phase under heat treatment. This suggests that the milling process can lower the temperature of the solid state reaction between $La(OH)_3$ and Fe_2O_3 to form $LaFeO_3$ perovskite.

For the sample after 50 h of milling time (Figure 3f), the first endothermic peak can still be clearly seen, with the peak temperature at 383 °C, while the second endothermic peak is not distinguished. The small exothermic peak with peak temperature ~ 667 °C can be assigned to the formation of $LaFeO_3$ perovskite. The TGA curve (Figure 3l) still shows two corresponding weight losses, with the values of -3.82% and -1.58%, respectively. The dramatic decreases in the two weight losses are due to the consumption of $La(OH)_3$ to convert to LaOOH and form $LaFeO_3$ perovskite after the long milling time. This is confirmed by the XRD results that the intensities of $La(OH)_3$ diffraction peaks dramatically decrease at this milling time scale, part of $La(OH)_3$ dehydrated to LaOOH and reacted with Fe_2O_3 to form $LaFeO_3$ perovskite.

The DSC and TGA curves of milled samples under impact mode are shown in Figure 4. Similar thermogravimetric results to those of shear mode milled sample were obtained. The intensities of the two endothermic peaks decrease with the milling time, and the corresponding weigh losses decrease, suggesting the consumption of $La(OH)_3$ phase and part of $La(OH)_3$ entering into Fe_2O_3 lattice. After 25 and 50 h milling time, the appearance of the small exothermic peak suggests that the milling process can lower the solid state reaction temperature between $La(OH)_3$ and Fe_2O_3. It has to be noted that no $La(OH)_3$ phase can be detected after 50 h of milling time (Figure 2f), while the DSC and TGA curves still show the two-step dehydration of $La(OH)_3$. Since no special care for the 50 h milled sample has been taken after the milling process, part of LaOOH phase may absorb moisture under ambient atmosphere and convert back to $La(OH)_3$ phase.

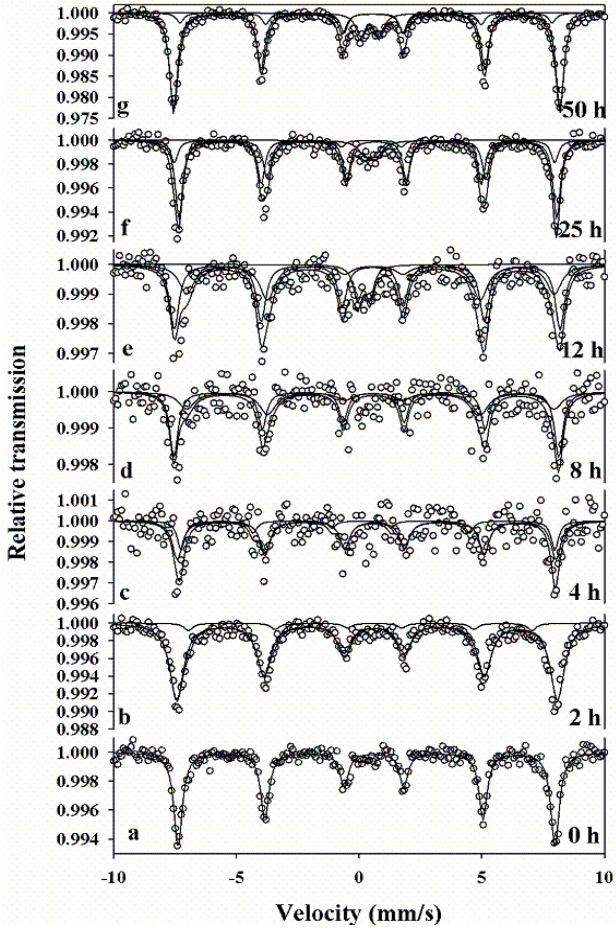

Figure 5. Mössbauer spectra of mixed La_2O_3-α-Fe_2O_3 samples in 1:1 molar ratio under shear mode and milling time of: (a) 0 hour; (b) 2 hours; (c) 4 hours; (d) 8 hours; (e) 12 hours; (f) 25 hours; (g) 50 hours, respectively.

3.3. Mössbauer Spectroscopy

Figures 5 and 6 show the room temperature transmission Mössbauer spectra of mixed La_2O_3-α-Fe_2O_3 oxides (1:1 molar ratio) after milling for 2, 4, 8, 12, 25, and 50 hours under shear and impact modes, respectively. The hyperfine parameters corresponding to these spectra are given in Table 1. For the physically mixed Fe_2O_3-La_2O_3 oxides, the Mössbauer spectrum can be only fitted with one sextet, with the values of hyperfine magnetic field (B), isomer shift (I.S.), and quodrupole shift (Q.S.) of 47.93 T, 0.458 mm/s, and -0.297 mm/s, respectively, representing the pure Fe_2O_3 phase (Figure 5a and Figure 6a).

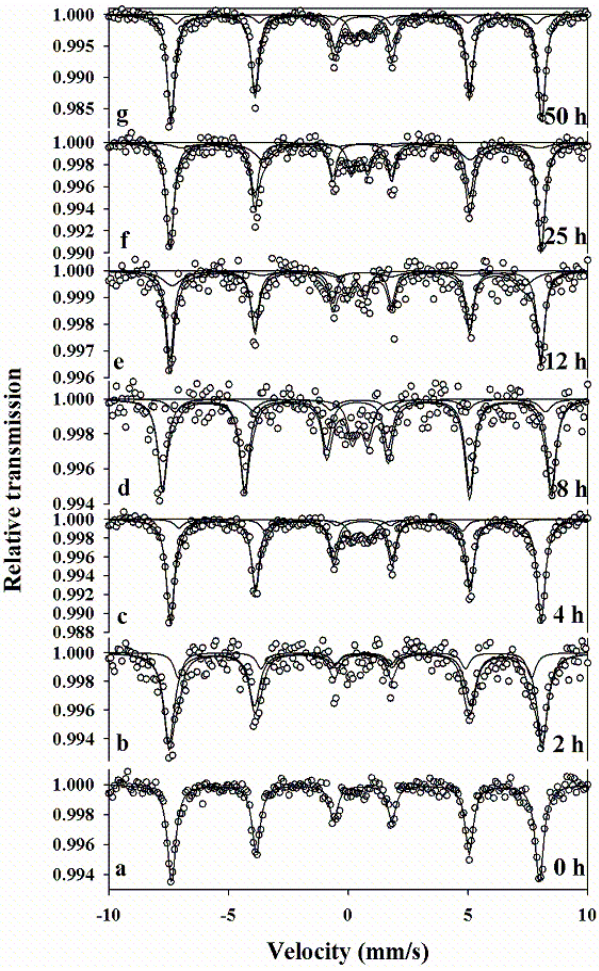

Figure 6. Mössbauer spectra of mixed La_2O_3-α-Fe_2O_3 samples in 1:1 molar ratio under impact mode and milling time of: (a) 0 hour; (b) 2 hours; (c) 4 hours; (d) 8 hours; (e) 12 hours; (f) 25 hours; (g) 50 hours, respectively.

For the sample at 2 h of milling time under shear mode (Figure 5b), the Mössbauer spectrum was fitted with 2 sextets, indicating the La^{3+} substitution of Fe^{3+} in the α-Fe_2O_3 lattice; the relative abundance of the magnetic phase with highest hyperfine magnetic field (48.11 T) is 93.10%, and the relative population of the magnetic phase with a lower hyperfine magnetic field of 46.42 T is 6.90%. Similar Mössbauer spectra with 2 sextets are observed for 4 and 8 h milled samples. After 12 h of milling time, the Mössbauer spectrum was fitted with 2 sextets and 1 doublet (Figure 5e). The small doublet, with isomer shift and quadrupole splitting values of 0.478 and 0.484 mm/s, respectively, has a population of 9.38%, and can be assigned to nonmagnetic phase with Fe^{3+} substitution of La^{3+} in the $La(OH)_3$ lattice. The appearance of the doublet occurs after only 12 h of milling time suggesting that it is more difficult for Fe^{3+} to enter the $La(OH)_3$ lattice than for La^{3+} to enter the Fe_2O_3 lattice.

Table 1. Mössbauer parameters for magneto-mechanical milled La_2O_3-α-Fe_2O_3 samples in 1:1 molar ratio at different ball milling times (BMT)

Mode	BMT (h)	I.S. (mm/s)	Q.S. (mm/s)	B (Tesla)	Abundance (%)
Shear	**0**	0.458	-0.297	47.93	100
	2	0.470	-0.289	48.11	93.10
		0.338	-0.585	46.42	6.90
	4	0.470	-0.327	48.85	73.36
		0.227	-0.268	47.25	26.64
	8	0.447	-0.301	48.65	59.08
		0.532	-0.147	46.54	40.92
	12	0.443	-0.226	48.75	52.77
		0.530	-0.136	46.45	37.85
		0.478	0.484	/	9.38
	25	0.356	-0.279	48.03	28.64
		0.533	-0.356	47.83	62.35
		0.482	0.483	/	9.01
	50	0.440	-0.252	48.83	72.71
		0.436	-0.299	47.01	15.99
		0.438	0.758	/	11.38
Impact	**0**	0.458	-0.297	47.93	100
	2	0.453	-0.285	48.31	78.50
		0.452	-0.351	45.72	21.50
	4	0.464	-0.295	48.01	79.29
		0.348	-0.598	44.12	11.68
		0.565	0.671	/	9.03
	8	0.372	-0.010	50.36	72.88
		0.497	-0.013	47.98	14.04
		0.489	0.637	/	13.08
	12	0.444	-0.290	48.03	67.28
		0.319	-0.651	45.65	22.99
		0.347	0.727	/	9.73
	25	0.448	-0.278	48.08	68.41
		0.640	-0.245	46.35	21.27
		0.474	0.685	/	10.32
	50	0.463	-0.248	48.02	68.17
		0.492	-0.300	46.62	21.48
		0.586	0.681	/	10.35
	Errors	**+/-0.01**	**+/-0.02**	**+/-1.0**	**+/-0.1**

When part of La^{3+} substitutes Fe^{3+} in Fe_2O_3 lattice, ferro- and/or antiferromagnetic ordering among Fe^{3+} can still be induced by exchange interaction, which gives sextets in Mössbauer spectra with different hyperfine magnetic fields. However, when a small amount of Fe^{3+} substitution of La^{3+} in $La(OH)_3$ lattice is introduced, no ferro- and/or antiferromagnetic ordering among Fe^{3+} can be induced by exchange interaction, therefore, only a quadrupole doublet appears. The isomer shift of Fe^{3+} extracted from the doublet is a bit higher compared to the value of Fe^{3+} extracted from the sextet pattern of Fe_2O_3, and this may be attributed to the change of neighbors in these two cases.

After 25 and 50 h of milling time, the Mössbauer spectra can still be fitted with 2 sextets and 1 quadrupole split

doublet, respectively. From XRD pattern (Figure 1f) of 50 h milled sample, the trace of $LaFeO_3$ magnetic phase was detected, however, no dramatic change in Mössbauer spectrum can be observed. It has been reported that the Mössbauer spectra of $LaFeO_3$ can be fitted with different sets of sextets and doublets due to the wide distribution in $LaFeO_3$ particle size. $LaFeO_3$ crystallites prepared by citrate method in size of 70nm possessed an antiferromagnetic structure and only one sextet was needed for its fitting, while those of 12nm were the superposition of weaker antiferromagnetic structure and stronger superparamagnetic structure, such that broadened sextets and doublets were needed[28]. The weak ferromagnetic behavior for $LaFeO_3$ with particle sizes of ~ 40nm was also observed from the hysteresis measurements[14]. The Mössbauer spectrum of $LaFeO_3$ single phase prepared by mechanical milling method was also reported to be composed of a broadened sextet pattern and a broadened singlet[29], as the average hyperfine magnetic field is lower than that of bulk $LaFeO_3$ [30]. All these suggest that the Mössbauer spectra of $LaFeO_3$ materials possess different magnetic properties and can be fitted with different sets of sextets and doublets, due to the different preparation methods which lead to different distribution in particle sizes. Therefore, the Mössbauer spectrum of trace of amorphous $LaFeO_3$ phase may overlap with the La^{3+} substituted/un-substituted Fe_2O_3 phase and the Fe^{3+} substituted $La(OH)_3$ phase. The percentage of the doublet as shown in Table 1 (~ 10%) doesn't change much as a function of milling time, suggesting that the 10% may be the maximum amount of Fe_2O_3 which can enter $La(OH)_3$ lattice under present milling conditions.

The Mössbauer spectra of impact mode milled samples are shown in Figure 6. For the 2 h milled sample, only 2 sextets are needed to fit the Mössbauer spectrum (Figure 6b), representing the La^{3+} un-substituted/substituted Fe_2O_3 phase. After 4 h of milling time, an extra doublet is needed (Figure 6c), suggesting the Fe^{3+} substitution of La^{3+} in $La(OH)_3$ phase. The appearance of the doublet after 4 h of milling time for impact mode and 12 h for shear mode is in good agreement with the impact mode being more energetic than the shear mode. Similar to the shear mode, the percentage of the doublet, which is around 10%, doesn't change much as a function of milling time, confirming our previous assumption that 10% is the maximum amount that Fe^{3+} can enter $La(OH)_3$ lattice.

According to the XRD, DSC-TGA, and Mössbauer results of both shear and impact milling modes, the initial stage growth mechanism of $LaFeO_3$ perovskite through magneto-mechanical milling method follows these steps: first of all, as shown by the intensities and broadness of the XRD diffraction peaks, the particle sizes of starting materials $La_2O_3/La(OH)_3$ and Fe_2O_3 decrease as a function of milling time; secondly, La^{3+} substitution of Fe^{3+} in Fe_2O_3 lattice and ~ 10% Fe^{3+} substitution of La^{3+} in $La(OH)_3$ phase occur under milling process, which can be identified by the Mössbauer spectra with 2 sextets and 1 doublet; at last, the $La(OH)_3$ decomposes to LaOOH at longer milling time and the solid state reaction occurs between Fe_2O_3 and LaOOH leading to the formation of amorphous $LaFeO_3$ phase; further, milling process causes the completion of the solid state reaction and the formation of $LaFeO_3$ single phase with well-developed ABO_3-type perovskite crystalline structure, which has been identified from our conventional milling method.

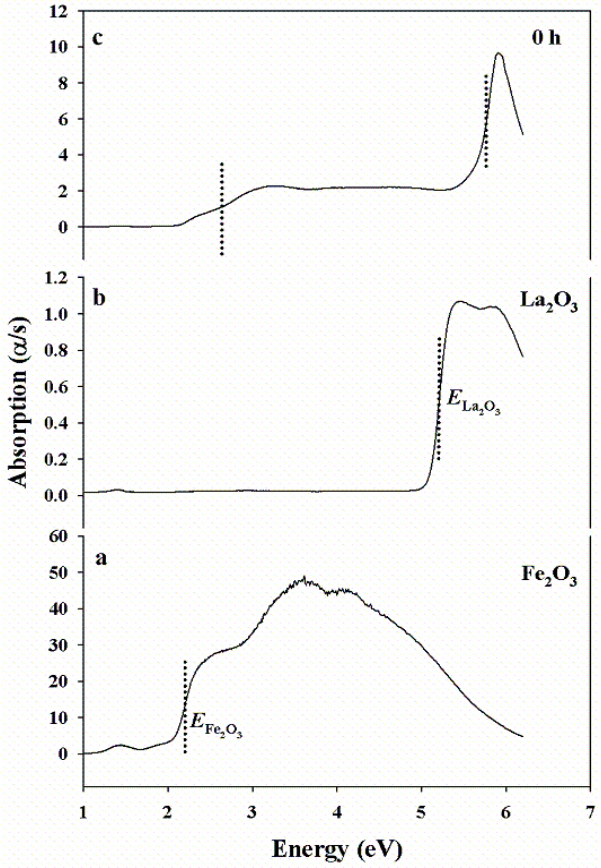

Figure 7. The optical diffuse reflectance spectrum converted to absorption for samples: (a) original Fe_2O_3, (b) original La_2O_3, and (c) physically mixed La_2O_3-α-Fe_2O_3 sample in 1:1 molar ratio at 0 hour of milling time. On the y axis, α is the absorbance and *s* is the scattering coefficient constant.

3.4. Optical Diffuse Reflectance Spectroscopy

The optical diffuse reflectance spectra for samples Fe_2O_3, La_2O_3, and La_2O_3-α-Fe_2O_3 (1:1 molar ratio) with 0 h of milling time are shown in Figure 7. For the Fe_2O_3, the valence and conduction bands arise from crystal field splitting of the Fe 3*d* levels due to the octahedral coordination of oxygen around Fe[31]. As shown in Figure 7a, diffuse reflectance spectra of original Fe_2O_3 exhibited a band gap energy value of ~ 2.2eV, which is consistent with reported value for bulk hematite[32-34]. Lanthanum (III) oxides have a structure in which lanthanum is seven-fold coordinated, with four short La-O bonds (2.30 Å) and three longer La-O bonds (2.70 Å). The band gap of La_2O_3 is indirect, and it has been recently reported it is in the range from 4.3eV to 6.0eV[34,35]. The valance band is at *Γ* and about 3.5eV wide. The conduction band minimum is due to the La *d* states. The density of states of La_2O_3 shows that valance band is strongly loca-

lized on O *p* states and the conduction band on La *d* with some La *s*, *p* states starting at 8eV[34]. The measured band gap energy of the lanthanum oxide has a value of ~ 5.2eV, the difference in band gap energy may arise from the coexistence of La_2O_3 and $La(OH)_3$ phases. For sample La_2O_3-α-Fe_2O_3 (1:1 molar ratio) with 0 h of milling time, i.e. just after the physically mixing of the hematite-lanthanum oxides, the band gap energy of Fe_2O_3 and lanthanum oxide shifted to higher energy levels, with values of ~ 2.60eV for Fe_2O_3 and ~ 5.76eV for lanthanum oxide, respectively. The variations in band gap energies of Fe_2O_3 and lanthanum oxide are attributed to the change in density of states of 2*p* level for O and 3*d* level for La and Fe. A similar change in band gap energy was also observed on Fe-doped TiO_2 system[36].

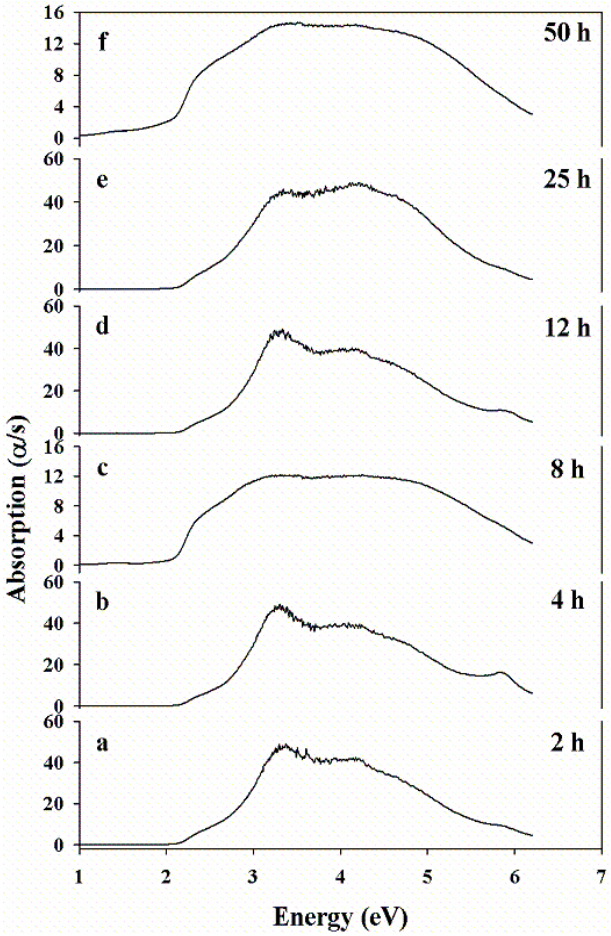

Figure 8. The optical diffuse reflectance spectrum converted to absorption for mixed La_2O_3-α-Fe_2O_3 samples in 1:1 molar ratio under shear mode and milling time of: (a) 2 hours; (b) 4 hours; (c) 8 hours; (d) 12 hours; (e) 25 hours; (f) 50 hours, respectively. On the y axis, is the absorbance and *s* is the scattering coefficient constant.

The optical diffuse reflectance spectra of shear mode milled samples are shown in Figure 8. For the sample under shear mode and after 2 h of milling time (Figure 8a), the band gap energy of the resulted sample is ~ 2.91eV, which is much higher than that of original Fe_2O_3 and slightly higher than that of Fe_2O_3 in the physically mixed hematite-lanthanum oxide sample. The change in band gap of Fe_2O_3 after milling process suggested the La^{3+} substitution of Fe^{3+} in Fe_2O_3 lattice, which is in good agreement with the Mössbauer results. No obvious band gap for La_2O_3 was observed due to the absorbent coefficients falling down and is very small in the wavelength range of UV-Vis light. No distinguishable change in the optical diffuse reflectance spectra was observed when the milling time was extended to 25 hours. It has been confirmed that $LaFeO_3$ perovskite was formed after 50 hours of milling under shear mode, however, no significant change was observed in the UV-Vis spectrum (Figure 8f). This is due to the similar band gap energies of Fe_2O_3 and the formed $LaFeO_3$ perovskite[37], as well as the band gap energy of $LaFeO_3$ phase being also ascribed to the electronic transitions from the valence band to conduction band (O_{2p}→Fe_{3d}, ~ 2.52eV). Therefore, the change in band gap energies of milled samples is mainly due to the gradual La^{3+} substitution of Fe^{3+} in Fe_2O_3 lattice.

Similar UV-Vis results were obtained for samples milled under the impact mode, with band gap of Fe_2O_3 shifted to higher energy after 2 hours of milling time. Extended milling time didn't cause further dramatic changes in UV-Vis spectra. All of the milled samples have band gap energies around 2.9eV.

4. Conclusions

The initial stage growth mechanism of $LaFeO_3$ perovskite was investigated through low energetic magneto-mechanical milling of La_2O_3 and Fe_2O_3 in stoichiometric ratios at room temperature. The La_2O_3 was highly hygroscopic and absorbed moisture under ambient atmosphere to form $La(OH)_3$ phase. XRD revealed that the average particle size of the $La(OH)_3$ and Fe_2O_3 decreased as a function of milling time. No solid state reaction to form $LaFeO_3$ took place when the milling time was less than 25 hours for both shear and impact modes. The detectable phase of $LaFeO_3$ perovskite was found only when magnetomechanical milling time was around 50 hours for the shear mode and 25 hours for the impact mode, with the simultaneous appearance of LaOOH phase. The DSC-TGA results suggested the two-step dehydration of the $La(OH)_3$ to LaOOH and then to La_2O_3. The decreases in intensities of endothermic peaks and the corresponding weight losses suggested that part of the $La(OH)_3$ entered the Fe_2O_3 lattice during the milling process. The Mössbauer spectroscopy studies showed that the spectrum of the milled La_2O_3-Fe_2O_3 composite consisted of two sextets and one doublet, indicating the La^{3+} substitution of Fe^{3+} into the Fe_2O_3 lattice, and small amounts of Fe^{3+} substitution of La^{3+} into the $La(OH)_3$ lattice under the milling process. The formation of $LaFeO_3$ occurs between nano-sized La^{3+} substituted/un-substituted Fe_2O_3 and the resultant LaOOH from dehydration of the $La(OH)_3$. Optical diffuse reflectance spectroscopy studies showed that all of the milled samples have semiconductor properties, with the band gap energies ~ 2.9eV. As compared to conventional milling, the magneto-mechanical milling method

offers access to studies of the very first stages of phase transformations in magnetic systems.

ACKNOWLEDGEMENTS

Thanks to Professor Jennifer A. Aitken (Chemistry Department, Duquesne University) for use of her UV/Vis/NIR instrument. This work was supported by the National Science Foundation under grant DMR-0854794.

REFERENCES

[1] Tejuca, L. G., Fireeo, J. L., and Tascón, J. M. D., 1989, Structure and reactivity of perovskite-type oxides., Adv. Catal., 36, 237-328

[2] Yamazoe, N., and Teraoka, Y., 1990, Oxidation catalysis of perovskites --- relationships to bulk structure and composition (valency, defect, etc.)., Catal. Today, 8, 175-199

[3] Arakawa, T., Kurachi, H., and Shiokawa, J., 1985, Physicochemical properties of rare earth perovskite oxides used as gas sensor material., J. Mater. Sci., 4, 1207-1210

[4] Traversa, E., Matsushima, S., Okada, G., Sadaoka, Y., Sakai, Y., and Watanabe, K., 1995, NO2 sensitive LaFeO3 thin films prepared by r.f. sputtering., Sens. Actuators B, 25, 661-664

[5] Asamitsu, A., Moritomo, Y., Tomioka, Y., Arima, T., and Tokura, Y., 1995, A structural phase transition induced by an external magnetic field., Nature, 373, 407-409

[6] Yao, T., Ariyoshi, A., and Inui, T., 1997, Synthesis of La-MeO_3 (Me = Cr, Mn, Fe, Co) perovskite oxides from aqueous solutions., J. Am. Ceram. Soc., 80, 2441-2444

[7] Kindermann, L., Das, D., Nickel, H., Hilpert, K., Appel, C. C., and Poulson, F. W., 1997, Chemical compatibility of $(La_{0.6}Ca_{0.4})_xFe_{0.8}M_{0.2}O_3$ with yttria-stabilized zirconia., J. Electrochem. Soc., 144, 717-720

[8] Stevenson, J. W., Armstrong, T. R., Carneim, R. D., Pederson, L .R., and Weber, W. J., 1996, Electrochemical properties of mixed conducting perovskites $La_{1-x}M_xCo_{1-y}Fe_yO_3$., J. Electrochem. Soc., 143, 2722-2729

[9] Cherry, M., Islam, M. S., and Catlow, C. R. A.,1995, Oxygen ion migration in perovskite-type oxides., J. Solid State Chem., 118, 125-132

[10] Belessi, V. C., Trikalitis, P. N., Ladavos, A. K., Bakas, T. V., and Pomonis, P. J., 1999, Structure and catalytic activity of $La_{1-x}FeO_3$ system (x=0.00, 0.05, 0.10, 0.15, 0.20, 0.5, 0.35) for the NO+CO reaction., Appl. Catal. A, 177, 53-68

[11] Gosavi, P. V., and Biniwale, R. B., 2010, Pure phase $LaFeO_3$ perovskite with improved surface area synthesized using different routes and its characterization., Mater. Chem. Phys., 119, 324-329

[12] Kondakindi, R. R., Kundu, A., Karan, K., Peppley, B. A., Qi, A. D., Thurgood, C., and Schurer, P., 2010, Characterization and activity of perovskite catalysts for autothermal reforming of dodecane., Appl. Catal. A, 390, 271-280

[13] Vázquez-Vázquez, C., Kögerler, P., López-Quintela, M. A., Sánchez, R. D., and Rivas, J., 1998, Preparation of $LaFeO_3$ particles by sol-gel technology., J. Mater. Res., 13, 451-456

[14] Sivakumar, M., Gedanken, A., Zhong, W., Jiang, Y. H., Du, Y. W., Brukental, I., Bhattacharya, D., Yeshurun, Y., and Nowik, I., 2004, Sonochemical synthesis of nanocrystalline $LaFeO_3$., J. Mater. Chem., 14, 764-769

[15] Giannakas, A. E., Ladavos, A. K., and Pomonis, P. J., 2004, Preparation, characterization and investigation of catalytic activity for NO + CO reaction of $LaMnO_3$ and $LaFeO_3$ perovskites prepared via microemulsion method., Appl. Catal. B, 49, 147-158

[16] Li, K. Y., Wang, D. J., Wu, F. Q., Xia, T. F., and Li, T. J., 1999, Studies on photoelectric gas-sensitive characters of nanocrystalline $LaFeO_3$. Mater. Chem. Phys., 60, 226-230

[17] Parida, K. M., Reddy, K. H., Martha, S., Das, D.P., Biswal, N., 2010, Fabrication of nanocrystalline $LaFeO_3$: An efficient sol-gel auto-combustion assisted visible light responsive photocatalyst for water decomposition., Int. J. Hydrogen Energy, 35, 12161-12168

[18] S. Kaliaguine, and A. Van Neste, "Process for synthesizing perovskite using high energy milling," U.S. Patent 6017504, 2000

[19] Szabo, V., Bassir, M., Van Neste, A., and Kaliaguine, S., 2002, Perovskite-type oxides synthesized by reactive grinding Part II: Catalytic properties of $LaCo_{(1-x)}Fe_xO_3$ in VOC oxidation., Appl. Catal. B, 37, 175-80

[20] Zhang, Q. W., and Saito, F., 2001, Effect of Fe_2O_3 crystallite size on its mechanochemical reaction with La_2O_3 to form $LaFeO_3$., J. Mater. Sci., 36, 2287-2290

[21] Cristóbal, A. A., Botta, P. M., Bercoff, P. G., and Port López, J. M., 2009, Mechanosynthesis and magnetic properties of nanocrystalline $LaFeO_3$ using different oxides., Mater. Res. Bull., 44, 1036-1040

[22] Kubelka, P., and Munk, F., 1931, Ein Beitrag zur Optik der Farbanstriche., Z. Tech. Phys., 12, 593-601. English translated by S. Westin

[23] Neumann, A., and Walter, D., 2006, The thermal transformation from lanthanum hydroxide to lanthanum hydroxide oxide., Thermochim. Acta, 445, 200-204

[24] Samata, H., Kimura, D., Saeki, Y., Nagata, Y., and Ozawa, T. C., 2007, Synthesis of lanthanum oxyhydroxide single crystals using an electrochemical method., Cryst. Growth, 304, 448-451

[25] Sorescu, M., Xu, T. H., and Diamandescu, L., 2010, Synthesis and characterization of $xTiO_2 \cdot (1-x)\alpha$-Fe_2O_3 magnetic ceramic nanostructure system., Mater. Character., 61, 1103-1118

[26] Wang, Y. P., Zhu, J. W., Zhang, L. L., Yang, X. J., Lu, L. D., Wang, X., 2006, Preparations and characterization of perovskite $LaFeO_3$ nanocrystals., Mater. Lett., 60, 1767-1770

[27] Khodaei, M., Enayati, M. H., and Karimzadeh, F., 2008, Mechanochemical behavior of Fe_2O_3-Al-Fe powder mixtures to produce Fe_3Al-Al_2O_3 nanocomposite powder., J. Mater. Sci., 43, 132-138

[28] Li, X., Cui, X. H., Liu, X. W., Jin, M. Z., Xiao, L. Z., and Zhao, M. Y., 1991, Mössbauer spectroscopic study on nanocrystalline $LaFeO_3$ materials., Hyperfine Interact. 69,

851-854

[29] Berry, F. J., Ren, X. L., Grancedo, J. R., and Marco, J .F., 2004, ^{57}Fe Mössbauer spectroscopy study of $LaFe_{1-x}Co_xO_3$ (x = 0 and 0.5) formed by mechanical milling., Hyperfine Interact., 156-157, 335-340

[30] Eibschütz, M., Shtrikman, S., and Treves, D., 1967, Mössbauer studies of Fe^{57} in orthoferrites., Phys. Rev., 156, 562-577

[31] Morin, F. J., 1954, Electrical properties of α-Fe_2O_3., Phys. Rev., 93, 1195-1199

[32] J. Robertson and P. W. Peacock, Materials Fundamentals of Gate Dielectrics, A. A. Demkov, and A. A. Navrotsky, Eds., Netherland, Springer, 2005

[33] Cheng, J. B., Li, A. D., Shao, Q. Y., Ling, H. Q., Wu, D., Wang, Y., Bao, Y. J., Wang, M., Liu, Z. G., and Ming, N. B., 2004, Growth and characteristics of La_2O_3 gate dielectric prepared by low pressure metalorganic chemical vapor deposition., Appl. Surf. Sci., 233, 91-98

[34] Thimsen, E., Biswas, S., Lo, C. S., and Biswas, P., 2009, Prediction the band structure of mixed transition metal oxides: theory and experiment., J. Phys. Chem. C, 113, 2014-2021

[35] Marusak, L. A., Messier, R., and White, W. B., 1980, Optical absorption spectrum of hematite, αFe_2O_3 near IR to UV., J. Phys. Chem. Solids, 41, 981-984

[36] Dare-Edwards, M. P., Goodenough, J. B., Hamnett, A., and Trevellick, P. R., 1983, Electrochemistry and photoelectrochemistry of iron (III) oxide., J. Chem. Soc. Faraday Trans., 79, 2027-2241

[37] Li, S. D., Jing, L. Q., Fu, W., Yang, L. B., Xin, B. F., and Fu, H. G., 2007, Photoinduced charge property of nanosized perovskite-type $LaFeO_3$ and its relationships with photocatalytic activity under visible irradiation., Mater. Res. Bull., 42, 203-212

.